

Right-Handed Neutrinos: DM and LFV vs Collider

Meziane Chekkal

Faculty of physics
University of Sciences and Technology of Oran Mohammed Boudiaf

Les XXXI Rencontres de Physique de la Vallée d'Aoste
March 7, 2017

Based on arXiv:1702.04399
in collaboration with A. Ahriche, A.B. Hammou, and S. Nasri

Class of Models & LFV Constraints

- In this work, we consider a class of radiative neutrino mass models that contain the following term in the Lagrangian [1, 2, 3, 4]

$$\mathcal{L}_N \supset -\frac{1}{2}m_{N_i}\overline{N_i^c}P_R N_i + g_{i\alpha}S^+\overline{N_i}\ell_{\alpha R} + \text{h.c.},$$

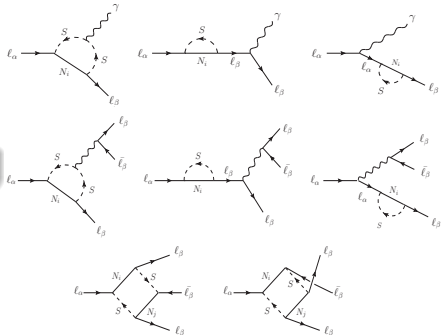
- These interactions can give rise to the LFV processes $\ell_\alpha \rightarrow \ell_\beta \gamma$ and $\ell_\alpha \rightarrow 3\ell_\beta$.
- We use the processes $\ell_\alpha \rightarrow \ell_\beta \gamma$ to calibrate the space parameters, their branching ratios is

$$\mathcal{B}(\ell_\alpha \rightarrow \ell_\beta \gamma) = \frac{3(4\pi)^3 \alpha}{4G_F^2} |A_D|^2 \times \mathcal{B}(\ell_\alpha \rightarrow \ell_\beta \nu_\alpha \bar{\nu}_\beta)$$

where

$$A_D = \sum_{i=1}^3 \frac{g_{i\beta}^* g_{i\alpha}}{2(4\pi)^2} \frac{1}{m_S^2} F \left(\frac{m_{N_i}^2}{m_S^2} \right),$$

$$F(x) = \frac{1-6x+3x^2+2x^3-6x^2 \log x}{6(1-x)^4}$$



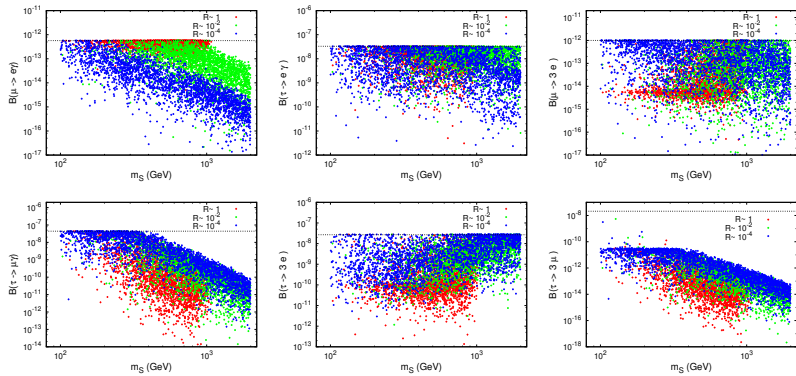
LFV process	Current bound
$\mu \rightarrow e\gamma$	5.7×10^{-13}
$\tau \rightarrow e\gamma$	3.3×10^{-8}
$\tau \rightarrow \mu\gamma$	4.4×10^{-8}
$\tau \rightarrow 3e$	1.0×10^{-12}
$\tau \rightarrow 3\tau$	2.7×10^{-8}
$\tau \rightarrow 3\tau$	2.1×10^{-8}

Class of Models & LFV Constraints

- Using process $\mu \rightarrow e\gamma$, we define the ratio R which makes possible to have larger yukawa coupling,

$$R = \frac{|\sum_{i=1}^3 g_{ie}^* g_{i\mu} F(x_i)|^2}{Max[|g_{ie}^* g_{i\mu} F(x_i)|^2]}$$

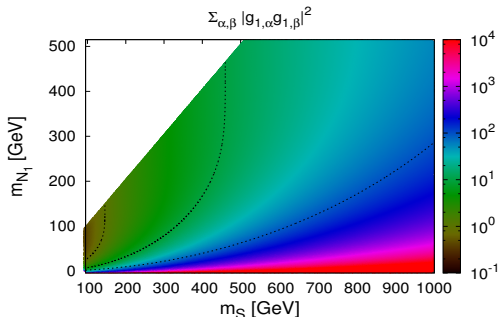
- 3 cases are considered, $R_1 \approx 1$ for a random generation without constraint, $R_2 \approx 10^{-2}$ for a moderate constraint and $R_3 \approx 10^{-4}$ for a strong constraint.



Relic Density constraint

- The lightest RH neutrino N_1 is stable and could be a good dark matter candidate.
- The relic density at the freeze-out is given by [5]

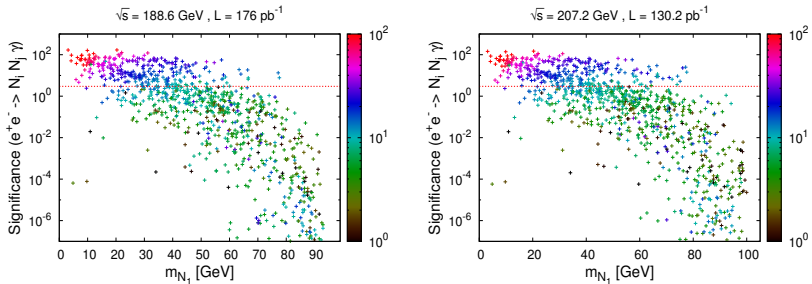
$$\Omega_{N_1} h^2 \simeq \frac{2x_f \times 1.1 \times 10^9 \text{ GeV}^{-1}}{\sqrt{g^*} M_{pl} \langle \sigma_{N_1 N_1} v_r \rangle} \simeq \frac{17.56}{\sum_{\alpha, \beta} |g_{1,\alpha} g_{1,\beta}^*|^2} \left(\frac{m_{N_1}}{50 \text{ GeV}} \right)^2 \frac{\left(1 + m_S^2/m_{N_1}^2 \right)^4}{1 + m_S^4/m_{N_1}^4}$$



- To satisfy both DM relic density and the current bounds on LFV processes, we must impose : $m_{N_1} < 200 \text{ GeV}$ and $m_S < 300 \text{ GeV}$ while keeping $m_{N_1} < m_S$

Constraint From LEP II

- $e^- e^+ \rightarrow \gamma + E_{miss}$ search by the L3 detector at LEP-II is considered, there are no events observed for significance higher than 3.
- We apply the same kinematical cuts used by L3 collaboration on mono-photonic channel $\{|cos \theta_\gamma| < 0.97, p_T^\gamma > 0.02\sqrt{s} \text{ and } E_\gamma > 1 \text{ GeV}\}$, use CalcHEP to generate the event of the signal and the background,



- A numerical constraint is extracted on space parameters of model,

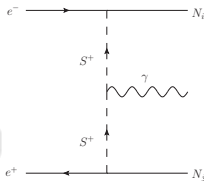
$$\text{Max}(|g_{i,e}|) < 0.66 \left[\frac{m_S}{100 \text{ GeV}} \right] \left[\frac{m_{N_i}}{50 \text{ GeV}} \right]$$



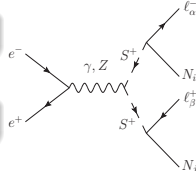
Possible Signatures At Lepton Colliders

- The main processes where the DM particles are in the final states are considered,

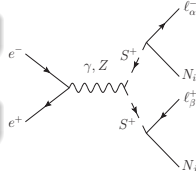
$$e^- e^+ \rightarrow \gamma + E_{miss}$$



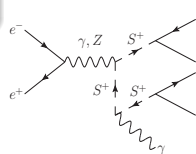
$$e^- e^+ \rightarrow S^+ S^- \rightarrow \ell_\alpha^+ \ell_\beta^- + E_{miss}$$



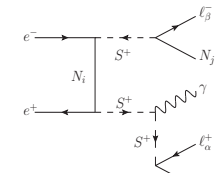
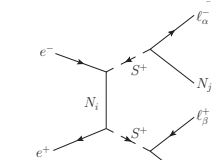
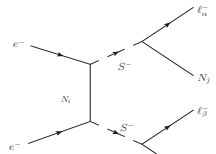
$$e^- e^- \rightarrow S^- S^- \rightarrow \ell_\alpha^- \ell_\beta^- + E_{miss}$$



$$e^- e^+ \rightarrow \gamma + S^+ S^- \rightarrow \gamma + \ell_\alpha^+ \ell_\beta^- + E_{miss}$$

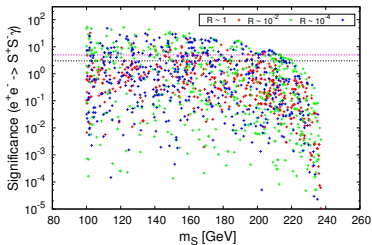
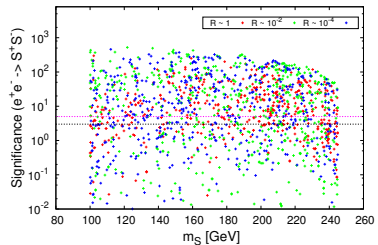
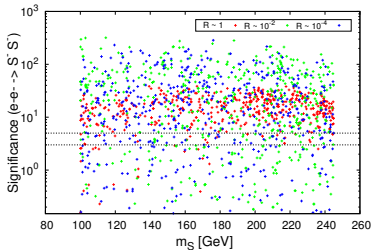
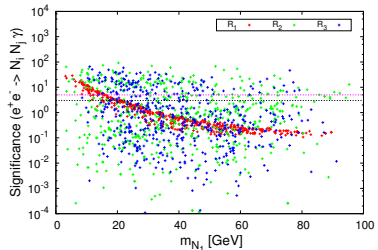


- All these processes are considered at $\sqrt{s} = 500 \text{ GeV}$ for a luminosity of 100 pb^{-1} .



Possible Signatures At Lepton Colliders

- The pre-cuts: $E_\gamma > 8 \text{ GeV}$ and $|\cos \theta_\gamma| < 0.998$ for the monophoton and $S^- S^+ + \gamma$ channels are imposed.



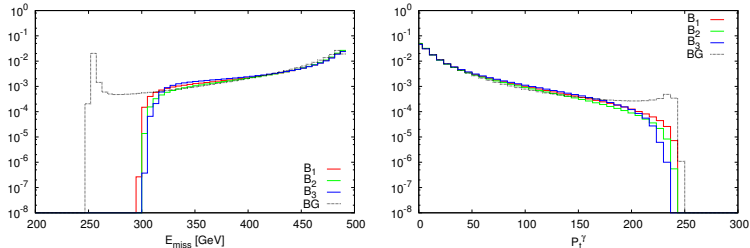
Benchmark Analysis

⇒ Three benchmark points selected from each R_i according to the fine-tuning degree

Point	$B_1(R_1)$	$B_2(R_2)$	$B_3(R_3)$
g_{1e}	$(7.506 + i0.014) \times 10^{-1}$	$(1.8284 + i0.103)$	$(-0.103 + i0.201)$
g_{2e}	$(-0.26819 - i1.5758) \times 10^{-4}$	$(1.543 + i3.004) \times 10^{-4}$	$(0.654 - i2.616) \times 10^{-2}$
g_{3e}	$(-1.360 - i0.707)$	$(0.313 - i0.549)$	$(-0.869 - i0.878)$
$m_S(\text{GeV})$	196.75	242.81	104.47
$m_{N_1}(\text{GeV})$	25.788	43.764	38.306
$m_{N_2}(\text{GeV})$	28.885	58.182	56.481
$m_{N_3}(\text{GeV})$	36.274	67.511	72.440

Using CalcHEP, we generate the distributions for different kinematic variables for both signal and background of the electron-positron

- The monophoton final state $\gamma + E_{miss}$

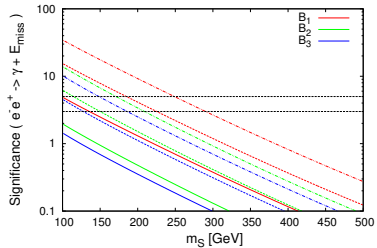


Benchmark Analysis

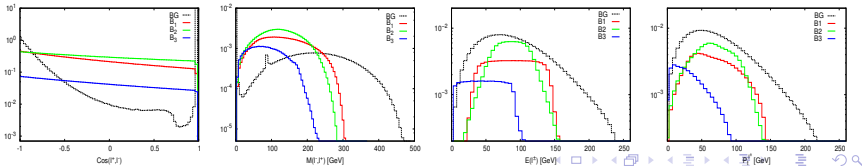
The monophotonic process cuts can be achieved as follows :

$$8 \text{ GeV} < E_\gamma < 300 \text{ GeV}, |\cos \theta_\gamma| < 0.998, E_{miss} > 300 \text{ GeV}$$

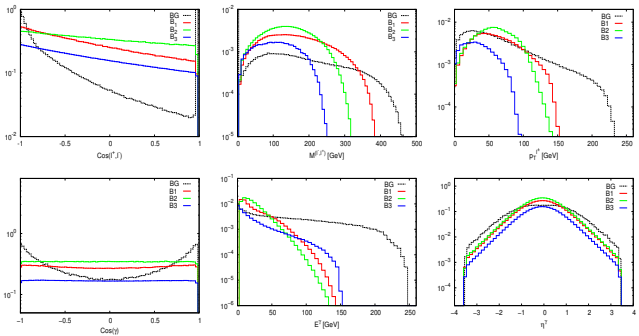
The significance is done at integrated luminosity of 10 (solid), 100 (dashed) and 500 (dash-dotted) fb^{-1}



- Final state $S^+S^- (\gamma)$



Benchmark Analysis



A similar generation to the monophoton is applied and the more relevant cuts are extracted as follows :

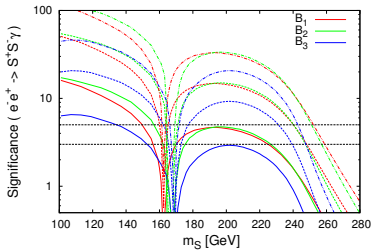
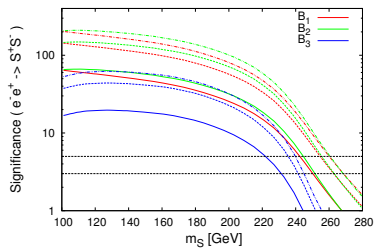
$$\text{Final state } S^+ S^- : \begin{cases} M_{\ell^+, \ell^-} < 300 \text{ GeV}, 150 \text{ GeV} < E_{miss} < 420 \text{ GeV}, \\ 30 \text{ GeV} < E^\ell < 180 \text{ GeV}, P_t^\ell < 170 \text{ GeV} \end{cases} \quad (1)$$

and

$$\text{Final state } S^+ S^- \gamma : \begin{cases} M_{\ell^+, \ell^-} < 300 \text{ GeV}, 150 \text{ GeV} < E_{miss} < 400 \text{ GeV}, \\ 30 \text{ GeV} < E^\ell < 170 \text{ GeV}, P_t^\ell < 170 \text{ GeV}, \\ |\cos(\theta_\gamma)| < 0.5, 8 \text{ GeV} < E^\gamma < 120 \text{ GeV}, P_t^\gamma < 110 \text{ GeV} \end{cases} \quad (2)$$

Benchmark Analysis

- The signal significance at integrated luminosity of 0.1 (solid), 0.5 (dashed) and 1 (dash-dotted) fb^{-1} for S^-S^+ and integrated luminosity of 1 (solid), 10 (dashed) and 50 (dash-dotted) fb^{-1} for $S^-S^+ + \gamma$.
- In these figures, a charged scalar is off-shell for $m_S > 250$ GeV and $m_S > 246$ GeV.



Analysis with Polarized Beams

- We re-analyze the processes discussed earlier by considering polarized beams as $P(e^-, e^+) = [+0.8, -0.3]$ while applying the same cuts used previously.

Process	$P(e^-, e^+)$	N_{BG}	BP	N_S	S_{10}	S_{100}	S_{500}
$e^- e^+ \rightarrow \gamma + E_{miss}$	[0,0]	46652	B_1	270.8	0.95	3.95	8.84
			B_2	250.32	1.16	3.65	8.17
			B_3	267.35	1.23	3.90	8.73
	[+0.8,-0.3]	6541	B_1	633.62	7.48	23.65	52.89
			B_2	585.74	6.94	21.94	49.06
			B_3	626.45	7.40	23.40	52.32

Process	$P(e^-, e^+)$	N_{BG}	BP	N_S	S_1	S_{10}	S_{50}
$e^- e^+ \rightarrow S^- S^+ + \gamma$	[0,0]	876.39	B_1	248.9	2.35	7.42	16.59
			B_2	91.22	0.93	2.93	6.56
			B_3	790.16	6.12	19.36	43.28
	[+0.8,-0.3]	123.20	B_1	555.53	6.74	21.32	47.68
			B_2	213.45	3.68	11.63	26.01
			B_3	1904	13.4	42.30	94.58

Conclusion

- *The production via electron-electron collision is huge compared to the background, this process is a clean and direct probe for RH neutrinos at the ILC*
- Monophotonic process is detectable at lepton colliders for a luminosity of a few hundred fb^{-1} and for charge scalars lighter than 200 GeV
- The production of a pair charged scalars without a photon in the final state the signal-to-background ratio can be very large for $m_S < 220 \text{ GeV}$ even at low integrated luminosity
- Final state $S^+ S^- \gamma$ is detectable at lepton colliders for a luminosity of a few tens fb^{-1} and for charge scalars lighter than 220 GeV
- *Using polarized beams we can improve the detectability of monophoton process to few tens fb^{-1} and to few fb^{-1} for The production of a pair charged scalars with a photon.*

-  A. Zee, Phys. Lett. **161B**, 141 (1985).
-  E. Ma, Phys. Rev. D**73**,077301(2006) [hep-ph/0601225].
-  L. M. Krauss, S. Nasri and M. Trodden, Phys. Rev. D**67**,085002(2003) [hep-ph/0210389].
-  H. Okada and K. Yagyu, Phys. Rev. D **93**, no. 1, 013004 (2016) [arXiv:1508.01046 [hep-ph]]. R. Tang and F. Zhang, Phys. Lett. B **741**, 163 (2015) [arXiv:1501.02020 [hep-ph]]. T. Nomura and H. Okada, arXiv:1610.04986 [hep-ph]. H. Okada and T. Toma, JCAP **1406**, 027 (2014) [arXiv:1312.3761 [hep-ph]]. S. Kashiwase, H. Okada, Y. Orikasa and T. Toma, Int. J. Mod. Phys. A **31**, no. 20n21, 1650121 (2016) Y. Orikasa, S. C. Park and R. Watanabe, PTEP **2016**, no. 12, 123B04 (2016) [arXiv:1512.09048 [hep-ph]].
-  A. Ahriche and S. Nasri, JCAP **1307**, 035 (2013) [arXiv:1304.2055 [hep-ph]].